ELSEVIER

Fuel Processing Technology 63 (2000) 125–147

FUEL PROCESSING TECHNOLOGY

www.elsevier.com/locate/fuproc

A model for the air emissions of trace metallic elements from coal combustors equipped with electrostatic precipitators

J.J. Helble *

Department of Chemical Engineering, University of Connecticut, 191 Auditorium Road, Box U-222, Storrs, CT 06269-3222, USA

Received 25 September 1998; received in revised form 9 September 1999; accepted 29 September 1999

Abstract

Trace element air emissions from pulverized coal combustion facilities are strongly element-dependent. Relatively non-volatile elements such as chromium and manganese are captured with efficiencies comparable to overall particulate capture, whereas more volatile elements such as selenium and arsenic are captured less efficiently than the ash particulate. Such element-specific behavior is a consequence of the partitioning of individual trace elements within the combustion and post-combustion environment, resulting in enrichment of the more volatile compounds in the smallest ash particles, coupled to size-dependent particulate penetration through air pollution control devices. In this paper, a model of trace element emissions that incorporates fundamental laboratory results on trace element partitioning as well as recent field emissions data is developed. Model results and comparison to field data indicate that while the emissions of non-volatile elements such as chromium are currently well predicted by existing database-referenced empirical models, predictions of the emitted concentrations of volatile compounds such as arsenic and selenium can be improved by more than 25% through incorporation of element and size-dependent partitioning and penetration.

Keywords: Air emissions; Trace elements; Coal combustion

1. Background

Pulverized coal combustion remains a significant anthropogenic source of trace metallic element emissions. Because the concentration of trace metals in coal is typically

* Fax: +1-860-486-2959; e-mail: helble@engr.uconn.edu

0378-3820/00/$ - see front matter
PII: S0378-3820(99)00093-4

Table 1
Trace metal enrichment in submicron fly ash particulate (elements identified in Title III of 1990 Clean Air Act Amendments, excluding Hg)
Key: Coal: B, bituminous; S, subbituminous; L, lignite; Br, brown coal; U, unspecified: ESP, electrostatic precipitator; FF, fabric filter (baghouse); APCD, air pollution control device (various); RE, relative enrichment factor as defined by Meij (1994) in Ref. [10]. RE = {(TE conc. in ash)(% ash in coal)}/(TE conc. in coal) RE > 3 considered enriched, a more restrictive definition than that adopted by Meij. TE, trace element; BA, bottom ash; FA, fly ash, either extractively sampled at the inlet to an air pollution control device, or removed from ESP hoppers; [c] f(dp), concentration measured as function of particle size, I at ESP or APCD inlet, O at ESP or APCD outlet; (b), beneficiated coal; SR, stoichiometric ratio.
Coal source information listed as nation, state (US), or region of origin as specified in cited reference.
Elements not listed were either not measured, or presented RE: $1.5 < RE < 3$.
Table represents expansion and reclassification of studies summarized by Linak and Wendt [39].

Coal type/source	Boiler size	Enriched	No trend or depleted	Method	Ref. (citation)
Field studies					
B Ill./Ky.	290 MWe cyclone	Sb, As, Cd, Cr, Pb, Ni, Se	Co, Mn	[c] FA BA	Klein et al. [6]
B U	350 MWe	Sb, As, Pb, Se		[c] f(dp), ESP-O	Gladney et al. [7]
B Poland	17.2 kg/s	As, Cd	Mn, Ni	[c] FA BA	Kauppinen and Pakkan. [8]
B Colombia	350 MWe	As, Cd, Pb, Se	Cr, Ni	[c] FA BA	Sander [9]
B Russia/Can	250 MWe	As, Cd, Pb, Se	Cr, Ni	[c] FA BA	Sander [9]
B US	295 MWe	As, Cd, Pb, Se	Cr, Ni	[c] FA BA	Sander [9]
B US, Austral.	115–645 MWe	Sb, As, Se		RE FA BA	Meij [10]
B UK	2000 MWe station	As, Pb	Cr, Mn, Ni	[c] FA BA	Martinez-Tarazona, Spears [11]
B Illinois	U	As, Sb, Se	Cr, Ni, Mn	RE FA BA	Demir et al. [12]
B Poland	160, 113 MWe	As, Cd, Co, Pb, Se	Be, Cr, Mn, Ni	RE FA BA	Aunela-Tapola et al. [13]
S US	750 MWe	Sb, As, Se		[c] f(dp), APCD-O	Ondov et al. [14]
S US	160, 203, 654 kg/s	Sb, As, Se		[c] f(dp), APCD-O	Ondov et al. [15]
S US	520 MWe	Sb, As, Cd, Cr, Ni, Se	Mn	[c] f(dp), ESP-I	Markowski et al. [16]
S Wyoming	37.5 MWe	Sb, As, Ni, Se		[c] f(dp), FF-I	Shendrikar et al. [17]
S US	113 MWe	Sb, As, Se	Mn	[c] f(dp), APCD-I	Markowski and Filby [18]
S Spain	1050 MWe station	As, Se, Cd	Be, Cr, Mn, Ni	[c] f(dp), ESP-I	Querol et al. [19]
S Spain	1050 MWe station	Sb, As, Co, Pb, Ni, Cr		[c] f(dp), ESP ash	Querol et al. [19]

L Texas	U	As, Sb, Se	Mn	[c] FA BA	James and Acevedo [20]
Br, L Bulgaria	U	As	Cr, Pb, Ni	[c] FA BA	Vassilev [21]
L Greece	U	As		[c] f(dp), ESP ash	Bogdanovic et al. [22]
U	U	Sb, As, Cd, Cr, Pb, Ni, Se	Mn	[c] f(dp), FA	Davison et al. [23]
U	180 MWe	Sb, As, Pb, Se		[c] FA BA	Kaakinen et al. [24]
U	U	Sb, As, Cd, Pb, Se,	Mn	[c] f(dp) ESP-O	Coles et al. [25]
U	500–700 MWe	As, Pb (Sb, Cr, Ni, Se also but data not shown)		[c] f(dp), ESP ash	Smith et al. [26]
U	U	As, Cr, Pb, Se	Mn	[c] f(dp), ESP ash	Smith et al. [27]
U	430, 750, 180 MWe	As, Se		[c] f(dp) ESP-O	Bierman and Ondov [28]
U	25 MWe	As, Ni	Se	RE f(dp) ESP-I	McElroy et al. [29]
Laboratory and pilot scale studies					
B Pittsburgh	Pilot 1. 5 MM Btu h^{-1}	Sb, As,Cd, Pb	Se	c f(dp), ESP-I	Tumati and Devito [30]
L No. Dakota	Lab 17 kW	As, Pb	Mn	RE f(dp)	Linak and Peterson [31]
Bench scale (drop tube) studies					
B, S, L US	20% O_2	Sb, As, Co, Cr, Mn		RE f(dp)	Quann et al. [32]
B Illinois (b)	10.5% O_2	As Sb	Cr, Co	[c] f(dp)	Helble [33]
B, S Pitt., Wyo.	SR 1.2	Sb, As, Cr, Se		[c] f(dp)	Bool and Helble [34]
S Wyoming	30% O_2	Mn, Cr		[c] f(dp)	Helble [33]
L Montana	20% O_2	Sb, As		[c] f(dp)	Neville and Sarofim [35]
L Montana	20% O_2	Sb, As, Cr, Co		[c] f(dp)	Quann et al. [36]
L Montana	20% O_2	Sb, As, Mn		[c] f(dp)	Haynes et al. [37]
L Montana	20% O_2	Sb, As, Cr		[c] f(dp)	Neville et al. [38]

in the 1–10 μg/g range [1,2], emissions from individual utility sources should remain well below the annual 10 ton per element major source threshold identified in the 1990 US Clean Air Act Amendments [3]. Nevertheless, the large quantities of coal consumed worldwide ensure that in aggregate, coal combustion contributes significantly to the total air burden of trace metals. Using 1983 emissions data from Western Europe, the United States, Canada, and the former Soviet Union, Nriagu and Pacyna [4] estimated worldwide trace metals emissions from a variety of sources. They concluded that electric utility coal combustion contributed 2 to 6% of the annual anthropogenic atmospheric arsenic emissions, 2–3% of the cadmium emissions, 14–17% of chromium emissions, 9–17% of the mercury emissions, 10–14% of the antimony emissions, and 6–13% of the selenium emissions. For each of these elements, anthropogenic sources constituted 40–85% of the total annual atmospheric emissions [5].

Trace elements are emitted from coal-fired utility sources as a consequence of vaporization during combustion. Volatile trace metals such as selenium and mercury are completely vaporized at combustion temperatures, and are sufficiently volatile to remain partly in the vapor phase as temperatures decrease through air pollution control devices and the stack. Other trace elements such as arsenic, antimony, and lead will partially vaporize at flame temperatures and subsequently condense on the surfaces of fly ash particles generated during combustion. For many trace elements, condensation leads to concentration enrichment in the submicron fly ash particle size range because of the high underlying surface area of this particulate. Studies of trace element partitioning conducted over the past 25 years have been consistent in reporting enrichment of selected elements in the submicron fly ash particulate. In Table 1, the findings of these studies are reported, grouped by coal type and the size of the facility in which measurements were made. Although most of these studies considered partitioning for a broad range of elements, results presented in Table 1 are restricted to the subset of elements listed in Title 3 of the Clean Air Act Amendments that are primarily emitted as part of the particulate matter. Antimony, arsenic, beryllium, cadmium, chromium, cobalt, lean, manganese, nickel, and selenium are therefore included in Table 1, whereas mercury is specifically excluded because of its emission primarily in the vapor phase. The results in Table 1 demonstrate that arsenic, antimony, lead, cadmium, cobalt, and selenium are nearly always enriched in the finest particulate, independent of the type of coal burned or the size of the combustion facility. In contrast, chromium and nickel show behavior that is dependent upon the rank of the parent coal. Whereas enrichment has been reported for sub-bituminous coals, it is infrequently reported for bituminous and lignitic coals. In many of the early field studies, possible contamination of particulate samples by stainless steel probes and impaction substrates has obscured interpretation of results for these elements [18,40]. More recent bench scale studies have suggested that rank-specific differences may, however, arise as a result of differences in the form-of-occurrence of chromium and nickel within specific coals [33]. Both elements may be present in mineral as well as the more volatile organic forms, and the limited available data suggest the existence of large coal to coal variations [41,42].

The enrichment of trace metals in submicron fly ash is potentially problematic because air pollution control equipment is generally less efficient in collecting particles less than 1 μm in size. Electrostatic precipitators (ESPs), used on 91% of the coal-fired

power plants in the US (corresponding to 91% of the coal-fired megawattage, Ref. [43]), have a collection efficiency minimum in the 0.1 to 1 um size range. Trace elements enriched in this size range will be captured with reduced collection efficiencies relative to the total particulate mass. Particulate emissions will therefore be enriched in some of these trace metallic species. This is seen in Table 2 for coal-fired power plants recently studied as part of Electric Power Research Institute (EPRI) and Department of Energy-sponsored programs in the United States. Only facilities utilizing an ESP for particulate control are represented. For elements such as arsenic and selenium, the metal capture efficiency is lower than the particulate capture efficiency. For others such as beryllium and manganese, metal capture efficiency is comparable to particulate capture efficiency.

Because the concentration of individual trace elements varies from coal to coal, and because the capture efficiency of trace elements differs from that of the particulate, predictive models to assess the level of trace element emissions from a given coal-fired facility are required. Such estimates are an important component of risk assessment studies that consider individual exposure to potentially hazardous air pollutants [43,44]. The simplest models are based on 'emissions factors' in which field data are collected and combined to yield an average emissions level for a particular fuel or unit type. Emission factors are generally reported on a mass per unit fuel consumption basis, and therefore do not account for the concentration of a trace element in a particular coal. Brooks [45] derived emissions factors from published field test data, but observed that the range of trace metal emissions was extremely broad. Brooks' findings are reported in Table 3 for selected elements. Emissions data span nearly four orders of magnitude for some elements. This is contrasted with the narrower range reported by Chow et al. in 1994 [40] for facilities measured as part of the EPRI-sponsored Power Plant Integrated Systems: Chemical Emissions Studies (PISCES) test program in the United States [40]. Data from the Brooks report shown in Table 3 were obtained by combining data from bituminous, sub-bituminous, and lignitic coals for both wet and dry bottomed pulverized coal fired utility plants equipped with electrostatic precipitators. Data in the Chow et al. study include facilities equipped with fabric filters as well as those equipped with

Table 2
Trace element capture efficiencies: field data (facilities utilizing ESP alone for particulate control)

Element	Average particulate capture efficiency	Average element capture efficiency	Ratio	Number of data points (sites)
Hg	99.1	28.9	0.291	17
Se	99.0	49.1	0.496	16
As	99.2	96.1	0.969	19
Cd	99.1	96.1	0.970	8
Pb	99.2	96.8	0.976	18
Ni	99.1	97.6	0.985	16
Cr	99.2	98.0	0.989	19
Co	98.9	98.2	0.992	11
Be	99.0	98.3	0.993	11
Mn	99.2	98.5	0.993	21
Sb	98.9	98.5	0.996	6

Table 3
Emissions factors for selected trace metals emitted by utility pulverized coal combustion (lb/10^{12} Btu) median (range)

	Brooks (1989)[a]	Chow et al. (1994)[b]
As	42 (0.17–242)	32 (6–120)
Cd	3.8 (0.22–52.8)	2 (0.06–8)
Cr	2300 (1.6–7970)	22 (9–45)
Mn	440 (1–9240)	–
Pb	44 (1.1–184)	12 (4–40)
Ni	2100 (70–5760)	15 (5–30)

[a] From Ref. [45]. Average of all coal types for utility boilers firing pulverized coal and utilizing electrostatic precipitators. Both wet and dry bottom units included in average. Individual boilers treated as single data points in deriving the table.
[b] From Ref. [40]. ESPs and fabric filters combined.

electrostatic precipitators. Chow et al. attributed the large differences in emission factors for chromium and nickel to the use of stainless steel sampling lines in many of the studies comprising the Brooks report.

A related method for predicting trace metal emissions incorporates capture efficiencies that are trace element specific, thus allowing coal-dependent variations in trace element concentrations to be examined. Capture efficiencies reported by Brooks [45] and Szpunar [46] are summarized in Table 4. The capture efficiencies reported by Szpunar are estimates for a new 500 MWe power plant with 99.8% particulate capture assumed. The values reported by Szpunar are closer to those obtained in the field testing programs of the early 1990s (Table 2), and thus are likely to represent reasonable estimates for a well-maintained power plant operating with high efficiency particulate control equipment.

The data reported by Szpunar incorporate trace element enrichment as a function of particle size by categorizing elements according to relative volatility [1,46]. While an improvement over the emission factors summarized in Table 3, the use of capture efficiencies neglects element-specific variations in volatility, and is restricted to providing estimates for facilities with comparable particulate control efficiencies. Rubin et al.

Table 4
Average capture efficiency for selected trace metals

	Brooks ESPs (1989)[a]	Szupnar (1993)[b]
As	87.5	97.2
Cd	74.6	97.3
Cr	71.5	99.0
Mn	78.1	98.0
Pb	–	98.2
Ni	79.1	99.6

[a] Data from Ref. [45].
[b] Data from Ref. [46].

[47] have incorporated the variability in field data by utilizing the distributions of measured trace element concentrations and capture efficiencies in the PISCES study to develop a probability-based emissions factor model. Results are reported as probabilistic outputs by specifying the percentage of facilities with a given set of input variables that would have emissions within a given range. Using a subset of approximately 12 data points to define the expected emissions range, the authors used the probabilistic model to predict emissions at one specific plant. Predicted means for chromium and selenium showed good agreement with measured emissions, whereas arsenic showed poor agreement.

While these models represent increasing levels of complexity, none incorporate the element specific vaporization occurring within the flame, nor do they address element-specific partitioning to different size classes of fly ash occurring downstream. Recognizing this, Meserole and Chow [48] improved upon the emission factor methodology by calculating hypothetical emissions for a trace metal compound based upon air pollution control device capture efficiency and trace element enrichment in the submicron fly ash (as a function of the fraction vaporized for a generic trace element). Rizeq et al. [49] later expanded this approach by adapting a model originally developed for waste incineration. In the Rizeq et al. model, trace element vaporization and condensation during coal combustion were explicitly treated by using equilibrium vapor pressures to determine the extent of vaporization of each element, and homogeneous and heterogeneous condensation to distribute the trace elements in the particulate phase. While this methodology represents a more fundamental and thus more general approach, there are limitations associated with the prediction of trace element vaporization using equilibrium thermochemistry. Previous studies have shown that mass transport and kinetic considerations affect vaporization rates and extents in coal ash systems [36,42,50], thus establishing the thermodynamic values as upper limits. Other factors can also limit the accuracy of thermodynamic partitioning models. For example, the formation of submicron ash particulate through the decomposition of pyrite minerals has been suggested [51]. This process may also contribute to the enrichment of trace elements such as arsenic in the submicron ash, a consequence of the frequent occurrence of arsenic within pyrite [41]. In addition, aluminosilicate mineral phases are typically neglected in calculating trace element vaporization and partitioning because of the scarcity of thermodynamic data for these compounds. Aluminosilicates are, however, important mineral phases in coal [42] and may contain substantial quantities of certain trace elements [41]. These limiting effects are best seen in equilibrium predictions that all of the lead, arsenic, antimony, and cadmium present in all coals will vaporize during combustion regardless of temperature or reaction stoichiometry [49]. The equilibrium model also predicts that chromium will vaporize completely under oxidizing conditions, but will show lower vaporization under locally reducing conditions. Bench scale measurements of chromium concentrations in the submicron ash would therefore be expected to show either no change or a decrease as particle temperature is increased. For arsenic and chromium, two elements for which recent bench data are available, the amount of each element present in the submicron fly ash (and taken to be indicative of the amount vaporized) is found to increase with increasing particle temperature [42], in contrast to the prediction of the thermodynamic approach.

A general model for trace element emissions must therefore be based upon fundamental trace element partitioning behavior within the combustion environment. It must address coal-specific trace element concentrations, element specific volatility, element specific partitioning among the different size classes of ash particles, and element and particle size-specific penetration through air pollution control devices such as the electrostatic precipitator. In this paper, a model that incorporates the framework of these fundamentally based efforts while utilizing experimental data to define elemental partitioning is described. The model further considers element-specific partitioning by utilizing models for heterogeneous condensation, surface reaction, or retention within the mineral phase that are element-specific and derived from fundamental combustion studies of trace element partitioning.

2. Model development

Extensive field data on trace element emissions recently obtained in DOE and EPRI-sponsored projects provides a large database that can be used to assess model predictions of trace element emissions. This database provides information on coal rank, ash content, sulfur content, trace element concentrations, coal higher heating value, trace element emissions rate, and particulate matter emissions rate for the ten trace elements listed in Table 1 at over 40 US sites. From this tabulated data, the capture efficiency of air pollution control devices for total particulate matter as well as individual trace metals can be derived. Comparison of these efficiencies provides a means for determining whether selected trace elements are preferentially emitted from coal-fired utility power plants, and whether there is any rank, control device, or facility-type dependence in such emissions.

The particulate collection efficiency of an air pollution control device is defined as

$$\eta = 1 - \mathrm{PM}_{\mathrm{out}}/\mathrm{PM}_{\mathrm{in}} \tag{1}$$

where $\mathrm{PM}_{\mathrm{out}}$ is the particulate matter concentration (mass per unit heat input, e.g., lb per million Btu) at the outlet of the air pollution control device, and $\mathrm{PM}_{\mathrm{in}}$ is the corresponding value at the inlet of the air pollution control device. $\mathrm{PM}_{\mathrm{out}}$ can be expressed in terms of coal parameters as

$$\mathrm{PM}_{\mathrm{out}} = \mathrm{PM}_{\mathrm{in}}(1-\eta) = f_{\mathrm{a}}(1-\eta)/H \tag{2}$$

where f_{a} is the mass fraction of ash in coal on an as-received basis, and H is the higher heating value of the coal on an energy content per unit mass basis. For any trace element i present in the coal, the emissions E_i on a mass per fuel energy content basis (e.g., lb trace element i per 10^{12} Btu) can be determined by analogy to Eq. (2),

$$E_i = A_{i,\mathrm{in}}(1-\eta_i) = C_i(1-\eta_i)/H \tag{3}$$

where $A_{i,\mathrm{in}}$ is the concentration of trace element i at the inlet to the air pollution control device (mass per unit fuel energy content), C_i is the concentration (mass fraction) of trace element i in the coal on an as received basis, and η_{i} is the capture efficiency of trace element i in the air pollution control device, defined as in Eq. (1). Combination of

Eqs. (2) and (3) yields an expression for trace element emissions as a function of measurable parameters:

$$E_i = \frac{C_i \mathrm{PM}_{\mathrm{out}}(1-\eta_i)}{f_{\mathrm{a}}(1-\eta)} \tag{4}$$

Thus, if trace element capture efficiency were correlated with particulate capture efficiency, a linear plot of E_i as a function of $(C_i\ \mathrm{PM}_{\mathrm{out}}/f_{\mathrm{a}})$ would pass through the origin with slope equal to $(1-\eta_i)/(1-\eta)$. Typically, however, a broad range is observed in emissions measurements made at different facilities. Modification of Eq. (4) to the empirical

$$E_i = a_i \left[\frac{(C_i \mathrm{PM}_{\mathrm{out}})}{f_{\mathrm{a}}} \right]^{b_i} \tag{5}$$

can also be considered, and is the form recommended by EPRI for interpretation of the DOE and PISCES data [52]. Although the large size of the underlying database makes it probable that the development of Eq. (5) for each trace metal will be more accurate than emissions factors proposed elsewhere (c.f. Tables 3 and 4), this approach remains a correlational one that does not account for the enrichment of many trace metals in the smallest particle sizes.

A more accurate model useful for predicting the emissions of trace metals from pulverized coal combustion sources equipped with electrostatic precipitators can be derived if trace element concentrations are predicted as a function of ash particle size, and if size-dependent particulate capture efficiencies are considered. Previous efforts have addressed these issues, but have used thermodynamic models for trace element vaporization [49] and have restricted consideration to homogeneous and heterogeneous condensation [48,49]. Fundamental bench scale studies have demonstrated, however, that minerals and trace elements transform through condensation as well as by surface reaction of vapor phase species with ash particles and by coalescence of ash particles within the burning coal char [33,37,39,53,54]. Trace element concentrations can therefore exhibit size dependence expressed as

$$CE_{i,j\,\mathrm{ash}} = k_{i,j}\mathrm{dp}_j^n \tag{6}$$

where $\mathrm{CE}_{i,j\ \mathrm{ash}}$ represents the concentration of trace element i in ash particles of size dp_j, $k_{i,j}$ is a proportionality constant, and n is the exponent representing the size dependence of concentration. The exponent n will equal -1 for heterogeneous condensation in the free molecular regime, -2 for heterogeneous condensation in the continuum regime, -1 for heterogeneous surface reaction control, and 0 for size-independent mass apportionment resulting from mineral coalescence [37,39,53]. Recall that in a previous model, Rizeq et al. treated only condensation, but allowed for size-regime dependent condensation flux [49,55]. Messerole and Chow incorporated a $1/\mathrm{dp}$ dependence in trace element concentration, which, although labeled as condensation, represents assumptions of condensation on the smallest submicrometer-scale ash particles (free molecular regime) and external surface reaction control on the larger fly ash particles (continuum regime) [48]. In the work described herein, the size dependence

was selected from mechanistic assessments derived from bench-scale experimental studies and is element-specific.

In order to predict trace element emissions, ash particle size distributions at the inlet to the electrostatic precipitator are needed. Models that predict the size distribution of fly ash particles formed during pulverized coal combustion are available, but require coal mineralogical data as input [56]. Because such data were not provided as part of any published field studies, site-specific calculation of fly ash particle size and composition distributions, a long-term goal of trace element emissions models [42], is not presently possible. Fly ash particle size distributions were therefore derived from field measurements of ash particle size distributions conducted at the inlet to a power station cold-side electrostatic precipitator. Measurements were conducted on two separate occasions, permitting sampling of ash during combustion of two bituminous coals [57]. Data were obtained by extractive sampling and subsequent size segregation using cyclones and a low pressure impactor (BLPI) yielding the size distributions shown in Fig. 1. An average particle size distribution at the ESP inlet was then obtained by averaging the distributions shown in Fig. 1 and renormalizing. In the 4- to 8-μm region where data collected by the cyclone and impactor overlapped, particle concentrations were considered additive. The fraction of ash in the submicron particle size range calculated from these combined data was 1.9%, comparable to the 0.5 to 2% observed in prior field studies [29,58,59]. Fly ash particle size distributions needed for the trace element emissions modeling were subsequently calculated for individual facilities by adjusting the mass in each size bin by the relative ash content of the fuel. The normalized fly ash particle size distribution (i.e., percentage of total fly ash mass within a given size range) remained fixed at the values derived from Fig. 1.

Particulate penetration through the electrostatic precipitator was determined through additional low pressure impactor and cyclone measurements at the electrostatic precipitator outlet at the same facility represented by the data in Fig. 1. Aluminum penetration

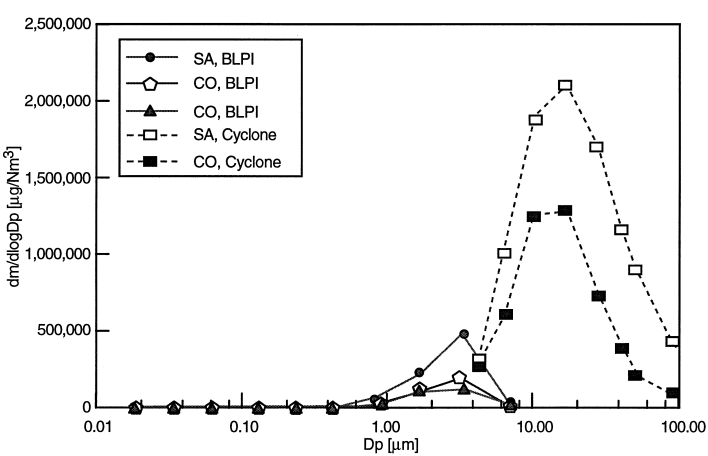

Fig. 1. Fly ash particle size distributions obtained from field measurements [57] and used to assign baseline size distribution at ESP inlet. CO represents Colombian coal, SA South African.

data [57] were used rather than total mass penetration data to avoid complications introduced by condensation and particle formation within cold-side ESPs [60]. The penetration curve derived from these measurements is presented in Fig. 2 along with other ESP penetration measurements from the published literature. In all studies, preferential penetration in the 0.1–1 μm size range was clearly observed. Data reported by McElroy et al. [29] demonstrate higher penetration, whereas 1998 data reported by Ylatalo and Hautanen [61] for combustion of a Polish coal are similar to the aluminum penetration data of Lind [57]. Mohr et al. [60] data are overall mass penetration data in the submicron regime for the two coals used to derive the aluminum data of Lind [57]. Although these data demonstrate higher penetration in the 0.1–0.6 μm range for the same two coals, evidence of particulate formation within the precipitator was observed. The aluminum data of Lind were therefore taken as being representative of particulate penetration through a well-operated current-generation ESP neglecting particle formation within the precipitator.

With the establishment of a fly ash particle size distribution at the electrostatic precipitator inlet, the distribution of trace elements as a function of ash particle size can be established. This was accomplished by defining the fraction of a trace element

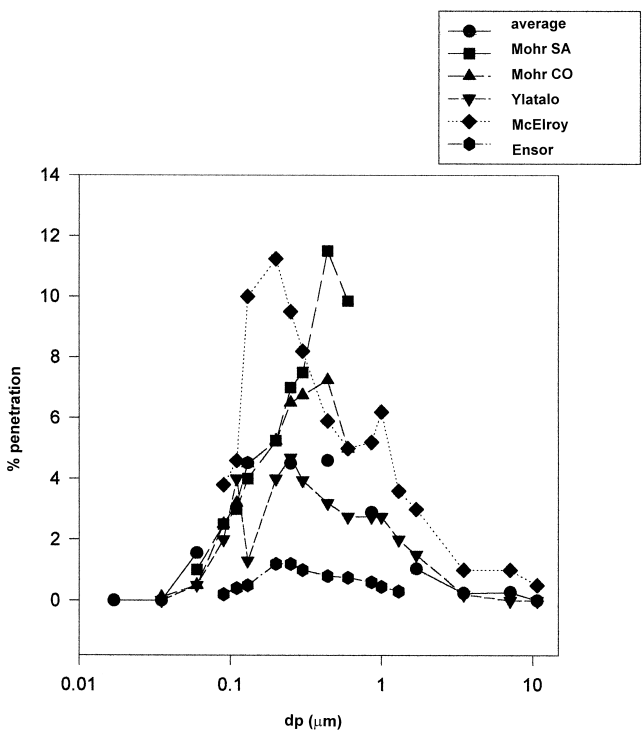

Fig. 2. Particle penetration through cold-side electrostatic precipitators as a function of particle size. Lind [57] data used in the model are reported for aluminum, all others are for total mass. Ylatalo and Hautanen [61] data are for the 234 MWe baseline case with all fields operative. Ensor et al. [64] data for hot-side ESP. Penetration peak at particle sizes less than 0.1 μm reported by Mohr et al. [60] excluded from figure.

associated with the submicron fly ash, and then distributing it among all fly ash particles as a function of particle size. Selenium, arsenic, and chromium were selected for detailed modeling because of differences in partitioning behavior observed at the bench scale. Selenium is a volatile element that may remain partially in the vapor phase at stack conditions. Arsenic is representative of a second type of volatile element that will vaporize significantly during combustion, but will condense completely before exiting the power plant. Based upon the field and bench studies summarized in Table 1, antimony, cadmium, cobalt and lead are expected to follow similar partitioning patterns. Chromium is representative of elements that are only partially volatile, with enrichment sensitive to coal type or combustion conditions. Nickel has demonstrated behavior similar to that of chromium in field and laboratory studies (Table 1). Based upon these observations and data from bench scale studies, the trace elements were distributed as indicated in Table 5. Particle size-dependent electrostatic precipitator penetration efficiencies were then used to determine the fraction of particulate and thus the fraction of trace element emitted.

Using these partition functions, trace element emissions from a given facility can be expressed as

$$E_{ijk} = \mathrm{Pt}_j\left[\mathrm{Pt}_k/\mathrm{Pt}_{\mathrm{baseline}}\right]\mathrm{CE}_{ijk} \tag{7}$$

where i represents a specific trace element, j represents a specific size (bin) of fly ash, k represents a specific utility boiler or site, E represents trace element emissions (mass per unit heat input of the fuel), Pt represents overall particulate mass penetration through the electrostatic precipitator, $\mathrm{Pt}_{\mathrm{baseline}}$ represents the overall particulate mass penetration through the baseline electrostatic precipitator (Fig. 2), and CE represents the concentration of the trace element in a specific size class of fly ash particles at the inlet to the electrostatic precipitator. Overall emissions of trace element i from site k can then be determined from the mass weighted sum over all size bins,

$$E_{ik} = \sum_j m_{jk} E_{ijk} \tag{8}$$

where m_{jk} represents the mass of fly ash in size bin j at site k. CE is a discontinuous function of particle size,

$$\mathrm{CE} = k_{1ik}\,\mathrm{dp}^n f_{v,i} \qquad \mathrm{dp} < 1\,\mu\mathrm{m} \tag{9a}$$

$$\mathrm{CE} = k_{2ik}\mathrm{dp}^n(1 - f_{v,i}) \qquad \mathrm{dp} > 1\,\mu\mathrm{m} \tag{9b}$$

where k_1 and k_2 are normalization constants and $f_{v,i}$ represents the fraction of trace element i associated with the submicron fly ash. Although size dependencies reported

Table 5
Partitioning functions used in development of emissions model

	Submicron	Supermicron
Chromium	Heterogeneous condensation	Coalescence (mass apportionment)
Arsenic	Surface reaction	Surface reaction
Selenium	Vapor + surface reaction	Surface reaction

for heterogeneous condensation are strictly valid only for particle sizes much greater than or less than the mean free path of the gas (approximately 0.1 μm at typical cold side ESP inlet temperatures of 140°C, and 0.4 μm at 1500°C), they are taken as being valid throughout the transition regime, with sharp transitions in mechanism occurring at a particle size of 1 μm. A cutoff size of 1 μm is convenient because experimental studies have assigned trace element volatility from the fraction of an element appearing in the submicron size range [32].

3. Results and discussion

An initial characterization of trace metal emissions can be obtained by applying Eqs. (1)–(5) to field data generated in the EPRI PISCES and DOE sampling programs. For example, examination of emissions data for arsenic shows broad scatter as shown in Fig. 3, indicating a lack of correlation between stack emissions E and the parameter C PM/fa specified by Eq. (4). The linear least squares correlation coefficient r^2 was determined to be 0.20 for 36 sites [42], with emissions ranging from less than 1 lb arsenic per 10^{12} Btu up to several hundred pounds per 10^{12} Btu. This clearly indicates that the emissions of arsenic are not simply correlated with particulate emissions for these facilities. An improved fit is obtained by using the empirical approach described by Eq. (5), however, as shown in Fig. 4. For arsenic, the r^2 value for the empirical equation was found to be 0.72. This observation of the empirical approach providing a better correlation to the field measurements was true for all ten of the trace elements considered in this study [42]. For arsenic, further improvement in the agreement between predicted and measured emissions was observed when the subset of facilities using fabric filtration for particulate control was considered ($R^2 = 0.92$). Because fabric filtration tends on average to capture submicron particulate with higher efficiency than does electrostatic precipitation, it is likely that much of the variability observed in Fig. 3 stems from the emission of small particulate enriched in arsenic.

The dependence of arsenic emissions on air pollution control device type further suggests that the approach outlined by Eqs. (6)–(8), (9a) and (9b) should be useful in improving emissions estimates for arsenic and other compounds with comparable combustion partitioning behavior. It is not clear, however, whether improved prediction would be obtained for less volatile elements such as chromium. The partitioning/penetration emissions model outlined by Eqs. (6)–(8), (9a) and (9b) was thus applied to chromium by generating emissions estimates and comparing them to data measured in the DOE and EPRI PISCES studies. The amount of chromium present in the submicron ash particle size range was used as an adjustable parameter to obtain the best fit to measured data. Goodness of fit was determined by minimizing the sum of squared residuals R, defined as

$$R_i = \sum_k \left(E_{ik,\,\text{predicted}} - E_{ik,\,\text{measured}} \right)^2 \tag{10}$$

A comparison of the model-predicted values of chromium emissions with those derived from Eq. (5), using an a_i value of 6.10 and b_i of 0.284 (both derived from EPRI

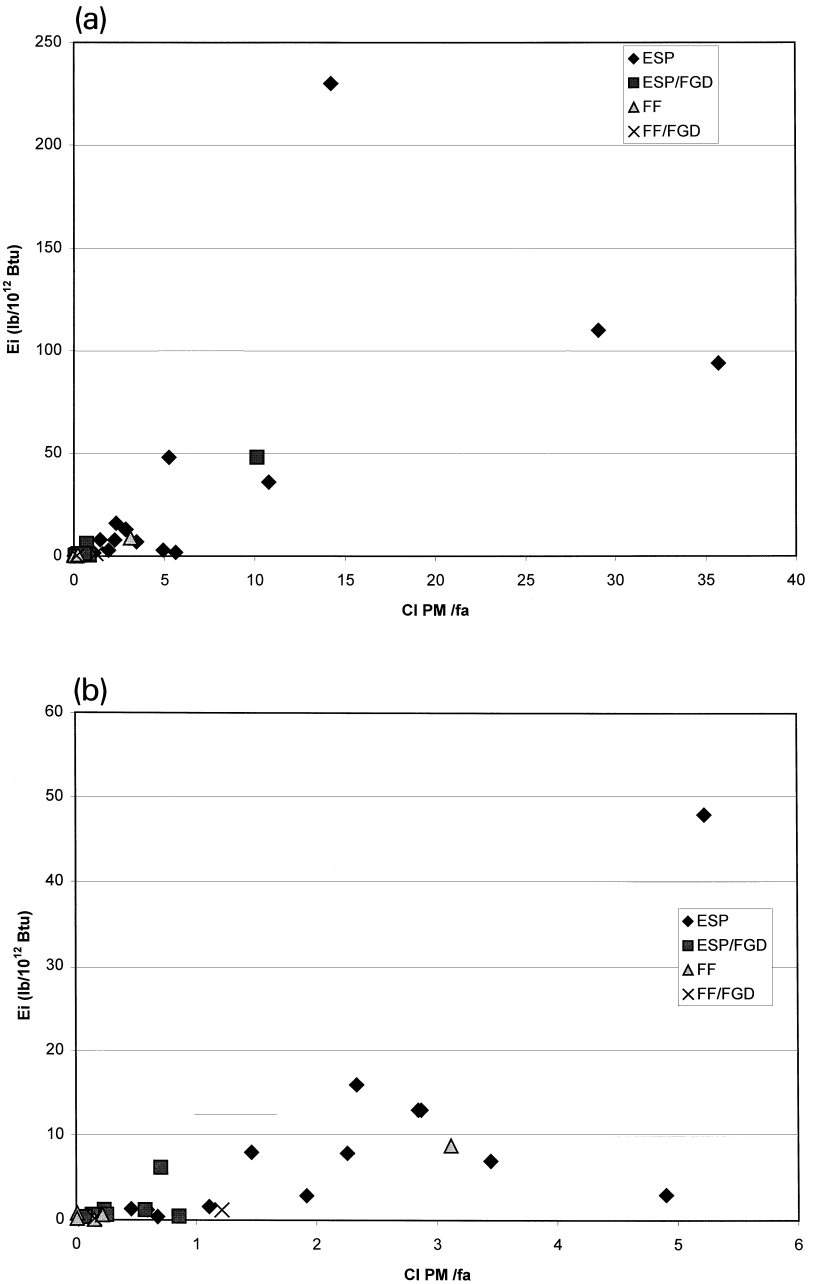

Fig. 3. Arsenic emissions data obtained from field measurements as a function of $C \times \mathrm{PM}/f_a$ as per Eq. (4). Different symbols represent different types of particulate control device. $R^2 = 0.20$ for these data. (a) entire dataset, (b) CI $\mathrm{PM}/f_a < 5$ only.

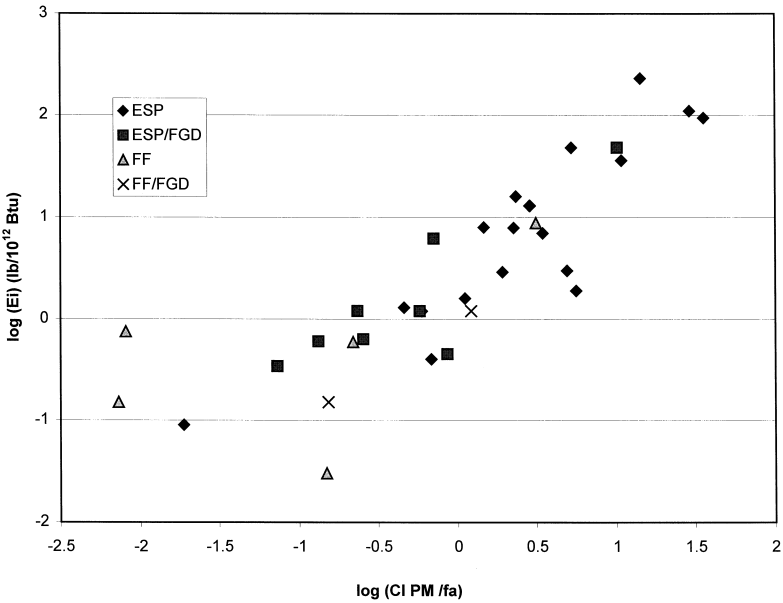

Fig. 4. Arsenic emissions data obtained from field measurements as a function of $C \times \mathrm{PM}/f_a$, plotted according to Eq. (5). Different symbols represent different types of particulate control device. $R^2 = 0.72$ for these data.

PISCES data for coal-fired facilities utilizing ESPs, with or without flue gas desulfurization) is shown in Fig. 5. The lower (solid) curve in the figure represents the empirical model, while the two broken lines represent the predictions of the penetration/partitioning model using two different mechanisms for distributing the chromium as a function

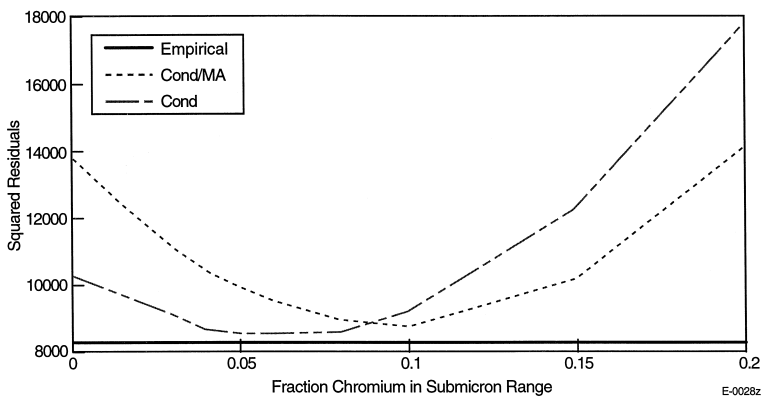

Fig. 5. Comparison of field measurements of chromium emissions with empirical model derived from database fit and partitioning/penetration model described by Eqs. (6)–(8), (9a) and (9b). COND represents condensation, MA mass apportionment.

of particle size. As expected from the formulation of the model, the partitioning/penetration approach shows a strong variation in agreement with field measurements as the fraction of chromium in the submicron particulate is varied. Best agreement with field data is obtained when the fraction of chromium in the submicron particulate is approximately 5–10%. As shown in Fig. 5, however, even at the minimum in either curve, the partitioning/penetration model does not predict the chromium emissions observed in field data any better than the empirical approach. This is attributed to the relatively low volatility of chromium; the less volatile an element is, the more evenly distributed an element will be as a function of fly ash particle size. A related factor contributing to the relative success of the empirical approach is believed to be the small percentage of sub-bituminous coal-fired boilers in the experimental dataset. In the discussion of Table 1 it was noted that chromium enrichment was only observed at field sites burning sub-bituminous coal. Examination of the limited sub-bituminous coal chromium emissions data in the EPRI/DOE database suggests similar results for facilities burning sub-bituminous coal as shown in Fig. 6. Given the dominance of bituminous coal-fired systems in the database, the influence of selective partitioning in sub-bituminous systems on the overall correlation is minimal. Bench scale experiments in which the amount of chromium in the submicron ash particulate correlated with the fraction of silicon in the submicron particulate, rather than the amount of chromium in the coal, provide further evidence in support of coal-specific chromium volatility [32].

Application of the model described in Eqs. (6)–(8), (9a) and (9b) to arsenic yields different results. Comparison of model-predicted arsenic emissions with those derived

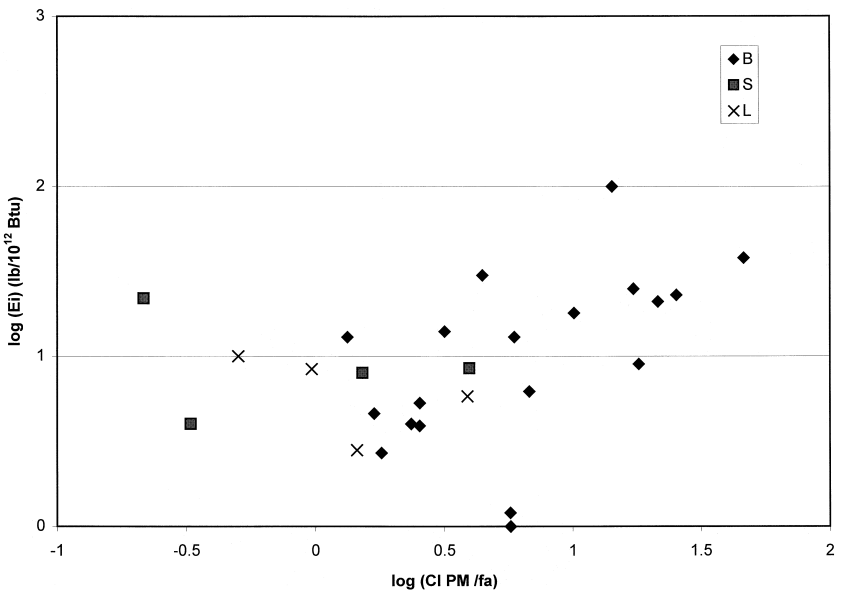

Fig. 6. Chromium emissions data obtained from field measurements as a function of $C \times \mathrm{PM}/f_a$ as per Eq. (4). Different symbols represent different coal rank as indicated. Data shown for facilities using ESP or ESP in conjunction with flue gas desulfurization only. $R^2 = 0.57$ for these data ($R^2 = 0.26$ using Eq. (4)). ♦: bituminous; ■: sub-bituminous; x: lignite.

from Eq. (5), using an a_i value of 3.14 and b_i of 0.887 is shown in Fig. 7. Again using the residuals as an indicator of agreement between field data and model prediction, it is seen that improved agreement is found for the partitioning/penetration model for fractions of arsenic in the submicron ash between 0.01 and 0.28. When the fractional partitioning of arsenic is set equal to 0.14, the minimum in the curve shown in Fig. 7, agreement with measurements is greater than 20% improved over that derived from empirical correlation of the field data. Predicted emissions based on particulate capture alone are also shown in Fig. 7; greater than 50% improvement in agreement with the data is observed for the partitioning model.

The arsenic fractional partitioning of 0.14 found by minimizing the difference between predicted and measured emissions in the available field data is consistent with reported experimental values. In Table 6, experimental partitioning data are provided for several trace elements. For arsenic, most data cluster between fractions of 0.10 and 0.42 in the submicron ash. Values determined in field measurements were generally lower than those observed in the laboratory, with an average value of 0.15 obtained from the four field measurements. Although the single bituminous coal field measurement yielded a value greater than those derived from the sub-bituminous coals, the extensive laboratory dataset reported by Quann et al. [32] did not identify any rank-specific differences for arsenic. The model fit value of 0.14 is thus within the range of reported partitioning values for arsenic, and is in good agreement with the small amount of data available from field measurements.

Using the penetration/partitioning model, arsenic emissions were predicted for three Canadian power plants comprising 12 boilers in total and representing units not

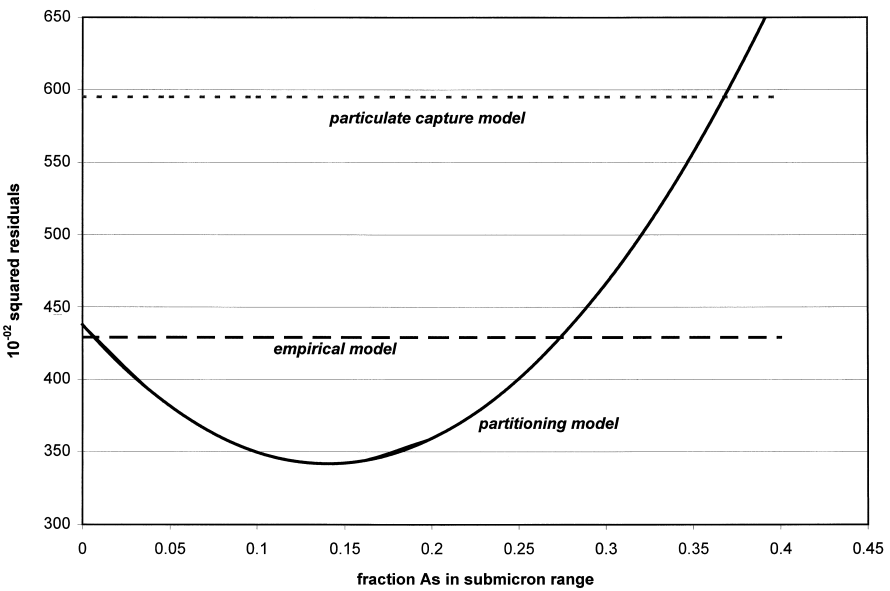

Fig. 7. Comparison of field measurements of arsenic emissions with (a) empirical model derived from database fit and (b) partitioning/penetration model described by Eqs. (6)–(8), (9a) and (9b).

Table 6
Fraction of trace element associated with submicron ash

Scale	Coal type	As	Sb	Cr	Mn	Cd	Se	Reference (citation no.)	Comment
Bench	B	33	36				67	Bool and Helble [34]	1 coal, all size fractions < 0.97 μm included
Bench	B	42[a]		2–24				Quann et al. [32]	4 coals, size segregated
Bench	B	20	23				16	Senior et al. [42]	3 coals
Bench	B + L	42[a]		12				Zeng [50]	Size segregated coals
Lab	B (I6)	10–12						Wendt et al. [63]	Illinois 6; all size fractions LE 0.535 μm
Lab	B (P8)	70						Wendt et al. [63]	Pittsburgh 8; all size fractions LE 0.535 μm
Pilot	B	20	32	1	12	61	42	Tumati and Devito [30]	Fraction present 'fine' mode $d_{mean} = 0.7$ μm
Field	B	10		6	3			Martinez-T. and Spears [11]	Total < 2.5 μm
Bench	S	18	22				19	Senior et al. [42]	1 coal
Bench	S	8	11				35	Bool and Helble [34]	1 coal, all size fractions < 0.97 μm included
Bench	S	42[a]		13–20				Quann et al. [32]	2 coals, size segregated
Bench	S	42[a]		35				Zeng [50]	3 coals, size segregated
Field	S	22	19	21	13			Shendrikar et al. [17]	Derived from dm/dlog(dp) data at FF inlet
Field	S	15	10	21	10			Ensor et al. [64]	Derived from dm/dlop(dp) at ESP inlet
Field	S	14	24		1		9	Markoswki and Filby [18]	Tabulated data
Bench	L	42[a]		7–15				Quann et al. [32]	3 coals, size segregated.

[a]Value derived from entire combined Quann et al. [32] and Zeng [50] database and therefore taken to be independent of coal type.

contained within the PISCES field testing database [62]. Emissions predictions were also made using the PISCES database-derived empirical parameters and by assuming that arsenic emissions were proportional to total particulate emissions. As shown in Fig. 8, the partitioning model provided the best agreement with measured emissions, with the sum of the residuals being at least 80% less than that derived from the other two models. A partitioning value of 0.14, signifying that 14% of the arsenic was associated with the submicron fly ash, was derived from the study of the PISCES database (Fig. 7) and used in this calculation.

Similar calculations were performed to assess selenium emissions for the facilities contained within the PISCES database. Meij [10], in a study of trace element emissions from a power station in the Netherlands burning a coal from the eastern US, reported that 25% of the selenium remained in the vapor phase at stack conditions. The partitioning model for selenium was thus modified to incorporate the fraction of vapor phase selenium as an adjustable parameter. Four values of the fraction of selenium in the vapor phase were considered: 0, 0.05, 0.10, and 0.20. As shown in Fig. 9, best agreement with experimental measurements was obtained for vapor fractions of 0.05–

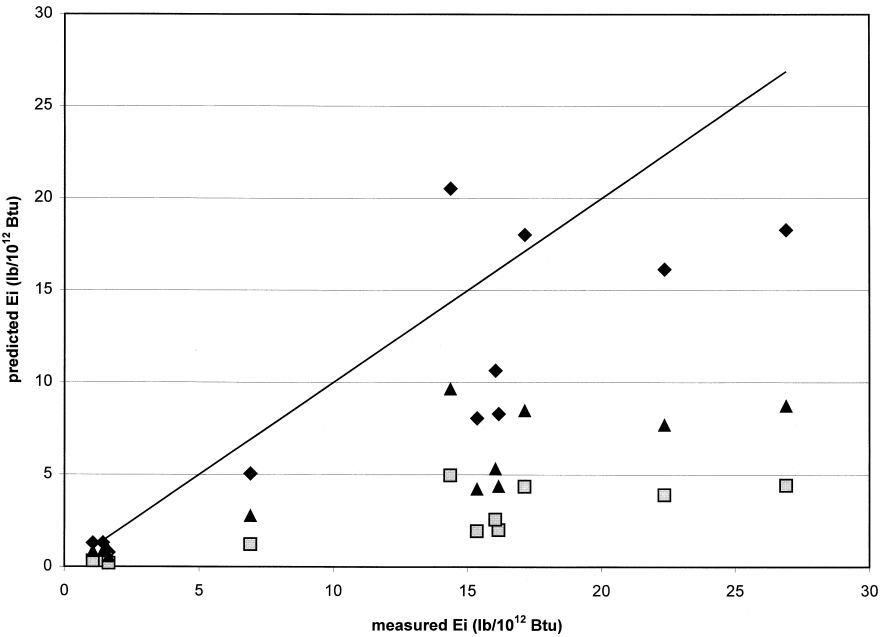

Fig. 8. Comparison of field measurements of arsenic emissions from twelve Canadian boilers with empirical model derived from database fit using US database (▲), model assuming trace element capture efficiency equals particulate capture efficiency ( ), and partitioning/penetration model described by Eqs. (6)–(8), (9a) and (9b) with $f_v = 0.14$ (◆).

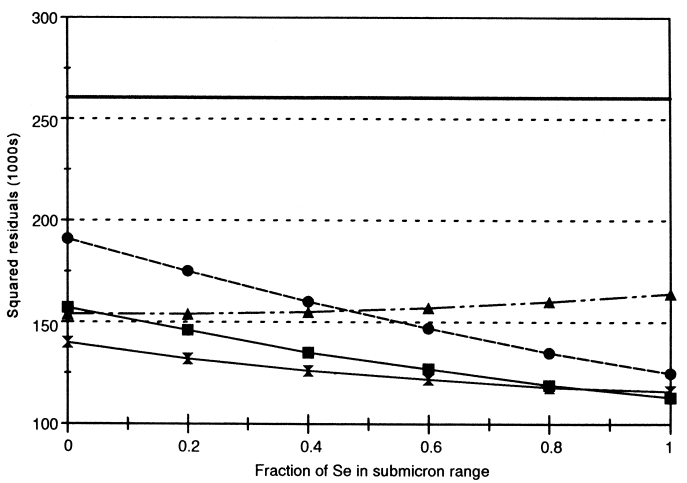

Fig. 9. Comparison of field measurements of selenium emissions with empirical model derived from database fit (solid line) and partitioning/penetration model described by Eqs. (6)–(8), (9a) and (9b), with ● 0% selenium vapor, ■ 5% vapor, ◆ 10% vapor, ⋈ 15% vapor; ▲ 20% vapor.

0.10, with 80% of the remaining selenium associated with the submicron ash particulate. At these optimum conditions, a 50% improvement in agreement (v. the empirical database-derived model) was obtained. Using a value of 20% vapor and 30% of the remainder in the submicron size range, consistent with the limited selenium partitioning data reported in Table 6, provided 40% improvement over the database-derived model. In either case, calculations indicate that improved emissions estimates could be obtained by considering size-dependent partitioning for this element.

4. Summary and conclusions

A model for the emission of trace elements from electric utility coal-fired power plants has been developed. The model partitions trace elements among fly ash particles as a function of ash particle size, and incorporates size-dependent particulate penetration through electrostatic precipitators to obtain emissions estimates. Comparison with recent field measurements and a database-derived model demonstrated that improved agreement with measured emissions levels could be obtained for relatively volatile elements such as arsenic and selenium. In contrast, agreement for chromium was comparable to that obtained with the database-derived model, and was attributed to the relatively low volatility of this element. A review of the literature in this area suggests that this conclusion may be restricted to facilities combusting bituminous coals, as facilities firing sub-bituminous coals generally produced greater fractions of chromium in the submicron ash particulate. The partitioning model might thus provide a more appropriate methodology for predicting chromium emissions for such facilities.

Although the fraction of an element in the submicron size range was treated as an adjustable parameter in this study, the values obtained for each of these elements were consistent with partitioning data reported in both field and laboratory studies. It is therefore concluded that for volatile elements such as arsenic and selenium, a model based upon partitioning and overall ESP capture efficiency offers the most accurate predictions of trace element emissions. Recommended values for arsenic are 14% in the submicron range, and for selenium, 20% vapor and 30% in the submicron fly ash size range. Further improvement in emissions prediction could be achieved by measuring the size-dependent particulate penetration though an ESP at an individual facility, but given the general absence of such data, the results presented herein suggest that an average value coupled to an overall particulate collection efficiency can provide improved predictions of trace element emissions. It is anticipated that first principles prediction of elemental partitioning, when coupled to the model presented herein, will provide the most accurate model of trace element emissions for all coals over a broad range of combustion conditions.

Acknowledgements

Ms. Terttaliisa Lind of the VTT Aerosol Technology Group generously provided ESP penetration data for aluminum as a supplement to her published work in this area.

Support for this work was provided by the US Department of Energy Federal Energy Technology Center and the Electric Power Research Institute.

References

[1] L.B. Clarke, L.L. Sloss, Trace Elements, Report No. IEACR/49, IEA Coal Research, London, 1992.
[2] M.S. Devito, L.W. Rosendale, V.B. Conrad, Comparison of trace-element contents of raw and clean commercial coals, Fuel Process. Technol. 39 (1–3) (1994) 87–106.
[3] United States Public Law 101-549, Amendments to the Clean Air Act, 101st Congress, 104 Statutes Part 4, 1990, 2399–2712.
[4] J.O. Nraigu, J.M. Pacyna, Quantitative assessment of worldwide contamination of air, water, and soils by trace metals, Nature 333 (1988) 134–139.
[5] J.O. Nriagu, A global assessment of natural sources of atmospheric trace metals, Nature 338 (1989) 47–49.
[6] D.H. Klein, A.W. Andren, J.A. Carter, J.F. Enery, C. Feldman, W. Fulkerson, W.S. Lyon, J.C. Ogle, Y. Talmi, R.I. Van Hook, N. Bolton, Pathways of thirty-seven trace elements through coal-fired power plant, Environ. Sci. Technol. 9 (10) (1975) 973–979.
[7] E.S. Gladney, J.A. Small, G.E. Gordon, W.H. Zoller, Composition and size distribution of in-stack particulate material at a coal-fired power plant, Atmos. Environ. 10 (1976) 1071–1077.
[8] E.I. Kauppinen, T.A. Pakkanen, Coal combustion aerosols: a field study, Environ. Sci. Technol. 24 (12) (1990) 1811–1818.
[9] B. Sander, Measurements of trace element mass balances in coal-fired power plants equipped with different types of FGD systems, Proceedings of the 2nd EPRI International Conference on Managing Hazardous Air Pollutants, Washington DC, July, 1993.
[10] R. Meij, Trace element behavior in coal-fired power plants, Fuel Process. Technol. 39 (1994) 199–217.
[11] M.R. Martinez-Tarazona, D.A. Spears, The fate of trace elements and bulk minerals in pulverized coal combustion in a power station, Fuel Process. Technol. 47 (1996) 79–92.
[12] I. Demir, R.E. Hughes, J.M. Lytle, K.K. Ho, Atmospheric emissions of trace elements at three types of coal-fired power plants, American Chemical Society Division of Fuel Chemistry Preprints 42 (1) (1997) 1101–1106.
[13] A. Aunela-Tapola, E. Hatanpaa, H. Hoffren, T. Laitinen, K. Larjava, P. Rasila, M. Tolvanen, A study of trace element behaviour in two modern coal-fired power plants: II. Trace element balances in two plants equipped with semi-dry flue gas desulphurization facilities, Fuel Process. Technol. 55 (1998) 13–34.
[14] J.M. Ondov, R.C. Ragaini, A.H. Biermann, Elemental particle size emissions from coal-fired power plants: use of an inertial cascade impactor, Atmos. Environ. 12 (1978) 1175–1185.
[15] J.M. Ondov, R.C. Ragaini, A.H. Biermann, Elemental emissions from coal-fired power plant. Comparison of a venturi wet scrubber system with a cold-side electrostatic precipitator, Environ. Sci. Technol. 13 (5) (1979) 598–607.
[16] G.R. Markowski, D.S. Ensor, R.C. Hooper, R.C. Carr, A submicron aerosol mode in flue gas from a pulverized coal utility boiler, Environ. Sci. Technol. 14 (11) (1980) 1400–1402.
[17] A.D. Shendrikar, D.S. Ensor, S.J. Cowen, G.J. Woffinden, M.W. McElroy, Size-dependent penetration of trace elements through a utility baghouse, Atmos. Environ. 17 (8) (1983) 1411–1421.
[18] G.R. Markowski, R. Filby, Trace element concentration as a function of particle size in fly ash from a pulverized coal utility boiler, Environ. Sci. Technol. 19 (9) (1985) 796–804.
[19] X. Querol, J.L. Fernandez-Turiel, A. Lopez-Soler, Trace elements in coal and their behaviour during combustion in a large power station, Fuel 74 (3) (1995) 331–343.
[20] W.D. James, L.E. Acevedo, Trace element partitioning in Texas lignite combustion, J. Radioanal. Nucl. Chem. 171 (2) (1993) 287–302.
[21] S.V. Vassilev, Trace elements in solid waste products from coal burning at some Bulgarian thermoelectric power stations, Fuel 73 (3) (1994) 367–374.
[22] I. Bogdanovic, S. Fazinic, S. Itskos, M. Jaksic, E. Karydas, V. Katselis, T. Paradellis, T. Tadic, O.

Valkovic, V. Valkovic, Trace element characterization of coal fly ash particles, Nucl. Instrum. Methods Phys. Res., Sect. B 99 (1995) 402–405.
[23] R.L. Davison, D.F.S. Natusch, J.R. Wallace, C.A. Evans Jr., Trace elements in fly ash: dependence of concentration on particle size, Environ. Sci. Technol. 8 (13) (1974) 1107–1113.
[24] J.W. Kaakinen, R.M. Jorden, M.H. Lawasani, R.E. West, Trace element behavior in coal-fired power plant, Environ. Sci. Technol. 9 (9) (1975) 862–869.
[25] D.G. Coles, R.C. Ragaini, J.M. Ondov, G.L. FIsher, D. Silberman, B.A. Prentice, Chemical studies of stack fly ash from a coal-fired power plant, Environ. Sci. Technol. 13 (4) (1979) 455–459.
[26] R.D. Smith, J.A. Campbell, K.K. Nielson, Characterization and formation of submicron particles in coal-fired plants, Atmos. Environ. 13 (1979) 607–617.
[27] R.D. Smith, J.A. Campbell, K.K. Nielson, Volatility of fly ash and coal, Fuel 59 (1980) 661–665.
[28] A.H. Biermann, J.M. Ondov, Application of surface deposition models to size-fractionated fly ash, Atmos. Environ. 14 (1980) 289–295.
[29] M.W. McElroy, R.C. Carr, D.S. Ensor, G.R. Markowski, Size distribution of fine particles from coal combustion, Science 215 (1981) 13–19.
[30] P.S. Tumati, M.S. Devito, Retention of condensed/solid phase trace elements in an electrostatic precipitator, Proceedings of the 1st EPRI International Conference on Managing Hazardous Air Pollutants: State of the Art, Washington DC, November, 1991.
[31] W.P. Linak, T.W. Peterson, Mechanisms governing the composition and size distribution of ash aerosol in a laboratory pulverized coal combustor, Proc. of the 21st Symposium (Int'l) on Combustion, The Combustion Institute, Pittsburgh, 1986, pp. 399–410.
[32] R.J. Quann, M. Neville, A.F. Sarofim, A laboratory study of the effect of coal selection on the amount and composition of combustion generated submicron particles, Combust. Sci. Technol. 74 (1990) 245–265.
[33] J.J. Helble, Trace element behavior during coal combustion: results of a laboratory study, Fuel Process. Technol. 39 (1994) 159–172.
[34] L.E. Bool III, J.J. Helble, A laboratory study of the partitioning of trace elements during pulverized coal combustion, Energy Fuels 9 (1995) 880–887.
[35] M. Neville, A.F. Sarofim, The stratified composition of inorganic submicron particles produced during coal combustion, Proc. of the 19th Symposium (Int'l) on Combustion, The Combustion Institute, Pittsburgh, 1982, pp. 1441–1449.
[36] R.J. Quann, M. Neville, M. Janghorbani, C.A. Mims, A.F. Sarofim, Mineral matter and trace element vaporization in a laboratory pulverized coal combustion system, Environ. Sci. Technol. 16 (11) (1982) 776–781.
[37] B.S. Haynes, M. Neville, R.J. Quann, A.F. Sarofim, Factors governing the surface enrichment of fly ash in volatile trace species, J. Colloid Interface Sci. 87 (1) (1982) 266–278.
[38] M. Neville, J.F. McCarthy, A.F. Sarofim, Size fractionation of submicrometer coal combustion aerosol for chemical analysis, Atmos. Environ. 17 (12) (1983) 2599–2604.
[39] W.P. Linak, J.O.L. Wendt, Toxic metal emissions from incineration: mechanisms and control, Prog. Energy Combust. Sci. 19 (1993) 145–185.
[40] W. Chow, M.J. Miller, I.M. Torrens, Pathways of trace elements in power plants: interim research results and implications, Fuel Process. Technol. 39 (1994) 5–20.
[41] R.B. Finkelman, Modes of occurrence of potentially hazardous elements in coal: levels of confidence, Fuel Process. Technol. 39 (1994) 21–34.
[42] C.L. Senior, L.E. Bool III, J.R. Morency, F.E. Huggins, G.P. Huffman, N. Shah, J.O.L. Wendt, F. Shadman, T.W. Peterson, W. Seames, B. Wu, A.F. Sarofim, I. Olmez, T. Zeng, S. Crowley, A., Kolker, C.A. Palmer, R.B. Finkelman, J.J. Helble, M.J. Wornat, Toxic substance from coal combustion — a comprehensive assessment, Physical Sciences Report No. PSI-1245/TR-1505 submitted to the US Department of Energy as the Final Report under contract DE-AC22-95PC95101, 1997.
[43] US Environmental Protection Agency, Study of Hazardous Air Pollutant Emissions from Electric Utility Steam Generating Units: Interim Final Report, Vol. 1, EPA Report Number EPA-453/R-96-013a, 1996.
[44] US Environmental Protection Agency, Study of Hazardous Air Pollutant Emissions from Electric Utility Steam Generating Units: Final Report, Executive Summary, Report to Congress, February, 1998.

[45] G. Brooks, Estimating air toxic emissions from coal and oil combustion sources, Radian Report to the US Environmental Protection Agency, EPA Report No. EPA-450/2-89-001, 1989.
[46] C.B. Szpunar, Projections of air toxic emissions from coal-fired utility combustion: input for hazardous air pollutant regulators, Proceedings of the 2nd EPRI International Conference on Managing Hazardous Air Pollutants, Washington DC, July, 1993.
[47] E.S. Rubin, M.B. Berkenpass, H.C. Frey, B. Toole-O'Neill, Modeling the uncertainty in hazardous air pollutant emissions, Proceedings of the 2nd EPRI International Conference on Managing Hazardous Air Pollutants, Washington DC, July, 1993.
[48] F.B. Meserole, W. Chow, Controlling trace species in the utility industry, Proceedings of the 1st EPRI International Conference on Managing Hazardous Air Pollutants: State of the Art, Washington DC, November, 1991.
[49] R.G. Rizeq, D.W. Hansell, W.R. Seeker, Predictions of metals emissions and partitioning in coal-fired combustion systems, Fuel Process. Technol. 39 (1994) 219–236.
[50] T. Zeng, Transformation of iron and trace elements during coal combustion, Sc.D. Thesis, Department of Mechanical Engineering, Massachusetts Institute of Technology, Cambridge MA, March, 1998.
[51] L.L. Baxter, R.E. Mitchell, The release of iron during the combustion of Illinois No. 6 coal, Combust. Flame 88 (1992) 1–14.
[52] Electric Power Research Institute, Electric Utility Trace Substances Synthesis Report, Report No. EPRI TR-104614, Project 3081, 1994.
[53] J.J. Helble, S. Srinivasachar, A.A. Boni, Factors influencing the transformation of minerals during pulverized coal combustion, Prog. Energy Combust. Sci. 16 (4) (1990) 267–280.
[54] M. Neville, A.F. Sarofim, The fate of sodium during pulverized coal combustion, Fuel 64 (1985) 384–390.
[55] R.G. Barton, W.D. Clark, W.R. Seeker, Fate of metals in waste combustion systems, Combust. Sci. Technol. 74 (6) (1990) 327–342.
[56] G. Wilemski, S. Srinivasachar, Prediction of ash formation in pulverized coal combustion with mineral distribution and char fragmentation models, in: J. Williamson, F. Wigley (Eds.), The Impacty of Ash Deposition on Coal Fired Plants, Taylor and Francis Publishers, London, 1994, pp. 151–164.
[57] T. Lind, Ash particle size distributions and electrostatic precipitator penetration data obtained in field measurements were generously provided by Ms. Terttaliisa Lind of the Aerosol Technology Group, VTT, Espoo Finland, Samples were obtained during 1994 measurements at the facility described by Mohr et al., 1996.
[58] E.J. Schulz, R.B. Engdahl, T.T. Frankenberg, Submicron particles from a pulverized coal fired boiler, Atmos. Environ. 9 (1975) 111–119.
[59] E.W. Schmidt, J.A. Gieseke, J.M. Allen, Size distribution of fine particulate emissions from a coal-fired power plant, Atmos. Environ. 10 (1976) 1065–1069.
[60] M. Mohr, S. Ylatalo, N. Klippel, E.I. Kauppinen, O. Riccius, H. Burtscher, Submicron fly ash penetration through electrostatic precipitators at two coal power plants, Aerosol Sci. Technol. 24 (1996) 191–204.
[61] S.I. Ylatalo, J. Hautanen, Electrostatic precipitator penetration function for pulverized coal combustion, Aerosol Sci. Technol. 29 (1998) 17–30.
[62] D. Orr, EPRI database compiled by Radian, Original data taken from J.C. Evans, K.H. Abel, K.B. Olsen, E.A. Lepel, R.W. Sanders, C.L. Wilkerson, D.J. Hayes, 1985, Characterization of trace constituents at Canadian coal-fired plants, Phase I — Final Report, Appendix H to K (data), Battelle Pacific Northwest Laboratories report to the Canadian Electrical Association, 1996.
[63] J.O.L. Wendt, S.D. Davis, T.K. Gale, W.S. Seames, Formation and control of semi-volatile toxic metals in combustion processes, Proc. 12th Members Conference, International Flame Research Foundation, Noordwijkerhout, The Netherlands, May 1998.
[64] D.S. Ensor, G. Markowski, G. Woffinden, R. Legg, S. Cowen, M. Murphy, A.D. Shendrikar, R. Pearson, R. Scheck, Evaluation of electrostatic precipitator performance at San Juan Unit number 1, Final Report submitted to the Electric Power Research Institute, report number EPRI CS-3252, Project 780-1, 1983.